JOM, Vol. 70, No. 7, 2018
https://doi.org/10.1007/s11837-018-2913-1

Structural Changes and Material Transport in Al_2O_3-Supported Cu/Fe Spinel Particles in a Simulated Chemical Looping Combustion Environment

W.H. HARRISON NEALLEY,[1,2] ANNA NAKANO,[1,3,4] JINICHIRO NAKANO,[1,3] and JAMES P. BENNETT[1]

1.—United States Department of Energy, National Energy Technology Laboratory, 1450 SW Queen Ave, Albany, OR 97321, USA. 2.—Oak Ridge Institute for Science and Education, 100 ORAU Way, Oak Ridge, TN 37380, USA. 3.—AECOM, P.O. Box 1959, Albany, OR 97321, USA. 4.—e-mail: anna.nakano@netl.doe.gov

Alumina-supported Cu/Fe spinel particles were exposed to oxidation/reduction atmospheres at 800°C. Structural changes of the particles subjected to gas cycles between air and 10 vol.% CO-90 vol.% Ar were studied from physical data and real-time images collected using a confocal scanning laser microscope equipped with a heating chamber. Overall particle volume slowly expanded with cycles while surface roughness decreased. Cross-sections of the exposed particles showed segregation of Cu and Fe to the edges of inner grains, which may have acted as oxygen carriers during the exposures. The particles remained whole during the cyclic exposures without any noticeable structural breakdown.

INTRODUCTION

The emission of CO_2 as a byproduct of carbon-based energy production is considered to be one of the main contributors to the amount of harmful greenhouse gases in the atmosphere. A number of efforts have been made to reduce the CO_2 released from industrial practices such as power plants, gasifiers, and smelters. Part of the core mechanism of CO_2 emissions lies with the oxidation of carbon in fossil fuels and with the use of air for combustion.

While air provides sufficient O_2 to support combustion, it is comprised largely of N_2. The N_2 chemically plays a minimal part in the combustion process but consumes a substantial amount of heat. Besides reducing the efficiency of the combustion process, the presence of N_2 makes the subsequent capture of CO_2 more difficult.

One way to alleviate N_2 issues is to use a process called chemical looping that produces pure CO_2 (without the presence of N_2) by utilizing oxygen carrier materials that exchange oxygen during oxidation/reduction (redox) cycles. The feasibility of this process may be limited if only liquid or gaseous carriers are considered. However, solid carriers would eliminate many of the technical and financial problems encountered when using more expensive, corrosive, or volatile substances.

The solid carrier materials would be more practical provided they remain stable over long periods of oxygen exchange cycles. Among multiple metals tested as an active component in solid carriers,[1] Cu and Fe were found to be of interest due to their high oxygen exchange capacity. Generally, to improve material durability, these metals are supported on ceramic materials such as Al_2O_3. However, at chemical looping operation temperatures < 1000°C, copper oxide and iron oxide react with Al_2O_3 to form aluminates,[2,3] which may slow the kinetics of the process. At the National Energy Technology Laboratory (NETL), a copper-iron spinel-based material supported on alumina (Al_2O_3) was developed as an oxygen carrier candidate for chemical looping applications[4] to address the problems mentioned above. Information of the real-time physical/chemical attrition of the particles, phase formation, or material segregation over redox gas cycles is essential for improvement of the oxygen carriers. In this work, real-time physical changes of this material during redox gas cycles at 800°C were

(Published online May 14, 2018)

investigated in situ using a controlled atmosphere, high-temperature, and confocal scanning laser microscope (CSLM). Chemical and structural changes occurring within the material are discussed based on scanning electron microscope analysis after such exposures.

MATERIALS AND METHODS

Chemical compositions of as-received alumina-supported copper-iron spinel particles developed at NETL were analyzed by x-ray fluorescence spectroscopy (Rigaku ZSX Primus II) and were found to contain (on an oxide basis) 31.19 mass% Al_2O_3, 37.49 mass% CuO, 31.32 mass% Fe_2O_3. The morphology and chemistry of the cross-sectioned spinel particles before and after exposures were analyzed by a scanning electron microscopy/energy-dispersive x-ray spectroscopy (SEM–EDX; FEI Inspect F and an Oxford INCA WAVE spectrometer). Spinel particles were prepared by a tumbling method. The majority of particles ranged between 500 μm and 1 mm, with the density of 2.9 g/cm^3, and 1 m^2/g surface area. More details on this material and its preparation can be found elsewhere.[5]

A CSLM (Olympus OLS3100) equipped with a heating chamber (Yonekura) was used to observe real-time high-temperature behaviors of spinel particles during isothermal oxidation–reduction gas cycles. A schematic of the controlled atmosphere heating chamber of the CSLM is shown in Fig. 1.

Samples placed in a high-density alumina crucible were set on a platinum holder connected to a type R thermocouple. Samples were heated by reflective heating using dual halogen lamps within a double-ellipsoid chamber lined with a thin layer of gold to maximize reflectivity. The geometry of the chamber focuses the heat from these lamps on a small volume of space in the center of the chamber. Reaction gases were introduced from above the sample. The microscope uses a laser with a wavelength of 408 $\pm$ 5 nm and a white light source; these were used to investigate real-time alterations of the sample's surface.

In-situ observations were conducted by first heating a sample to 800°C at 800°C/min in air (79 vol.% N_2-21 vol.% O_2). After holding at 800°C for 5 min, the air was switched to a reducing gas mixture of 10 vol.% CO-90 vol.% Ar (10CO-90Ar hereafter). Gas was introduced from immediately above the sample at a flowrate of 50 ml/min and the delay for the gas to reach the sample after opening the valve was estimated to be approximately 1.5 s from the thermocouple reading. No particle stirring was performed; sample evaluations were conducted in a static environment. Changes in morphology on the material's surface were recorded for 5 min in the reducing environment followed by a three-dimensional laser scan for up to 5 min. After a total of 10 min in 10CO-90Ar, the reaction gas was switched back to air and the same procedure (with 2.5 min hold and 5 min scan) was repeated while material changes were recorded throughout 10 redox cycles. At the end of the 10th cycle, the sample was quenched by turning off the heat and blowing He gas through the chamber at 60 ml/min, for post-exposure SEM analysis.

RESULTS AND DISCUSSION

Confocal Scanning Laser Microscopy

Three-dimensional representations of the spinel particles at 800°C during the oxidation periods were generated from confocal scan data (Fig. 2). Overall height and volume of the particles continuously increased as the cycles progressed. Small volume contractions, visually noted after initial expansion during each reduction period, were negligible compared to overall volume increase. After 10 cycles, the volume expansion was still ongoing; therefore,

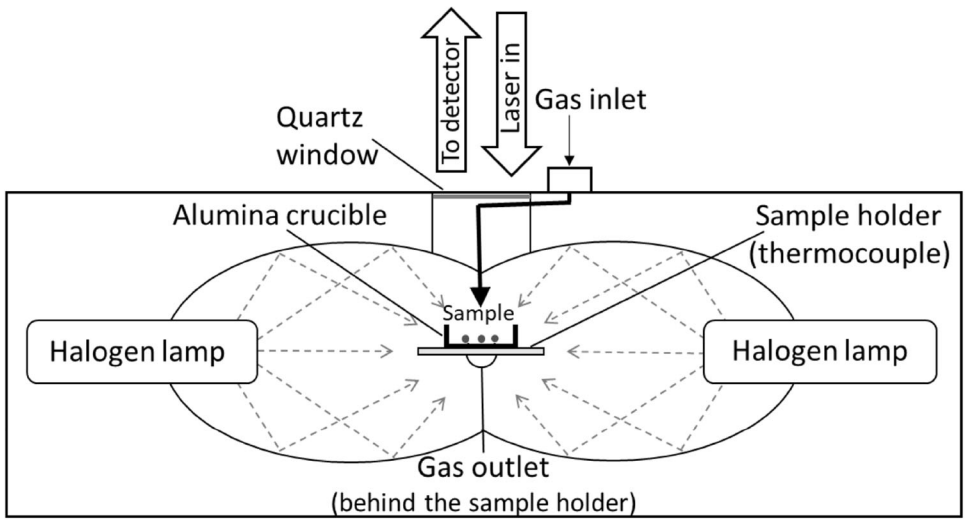

Fig. 1. A schematic of the CSLM heating chamber.

the projected volume change beyond 10 cycles cannot be ascertained from these data alone. By the end of cycle 10, the volume had increased by approximately 30% (Fig. 3). Note that this is a maximum value as hypothetical volumes below the widest portions of the particles were counted with those widths because they were not scanned from the top down. The particles exhibited sufficient durability under the static conditions. A drop in particle volume upon gas switch 1 (10CO-90Ar) was noted before it started to increase constantly with later cycles. A further study is underway to investigate the effects of individual gas switching.

The surface roughness, Sz, defined as the difference between the highest peaks and the lowest pits, was determined from the three-dimensional laser scan and is shown in Fig. 3. Measurements were conducted over an area of 250 μm $\times$ 250 μm on the

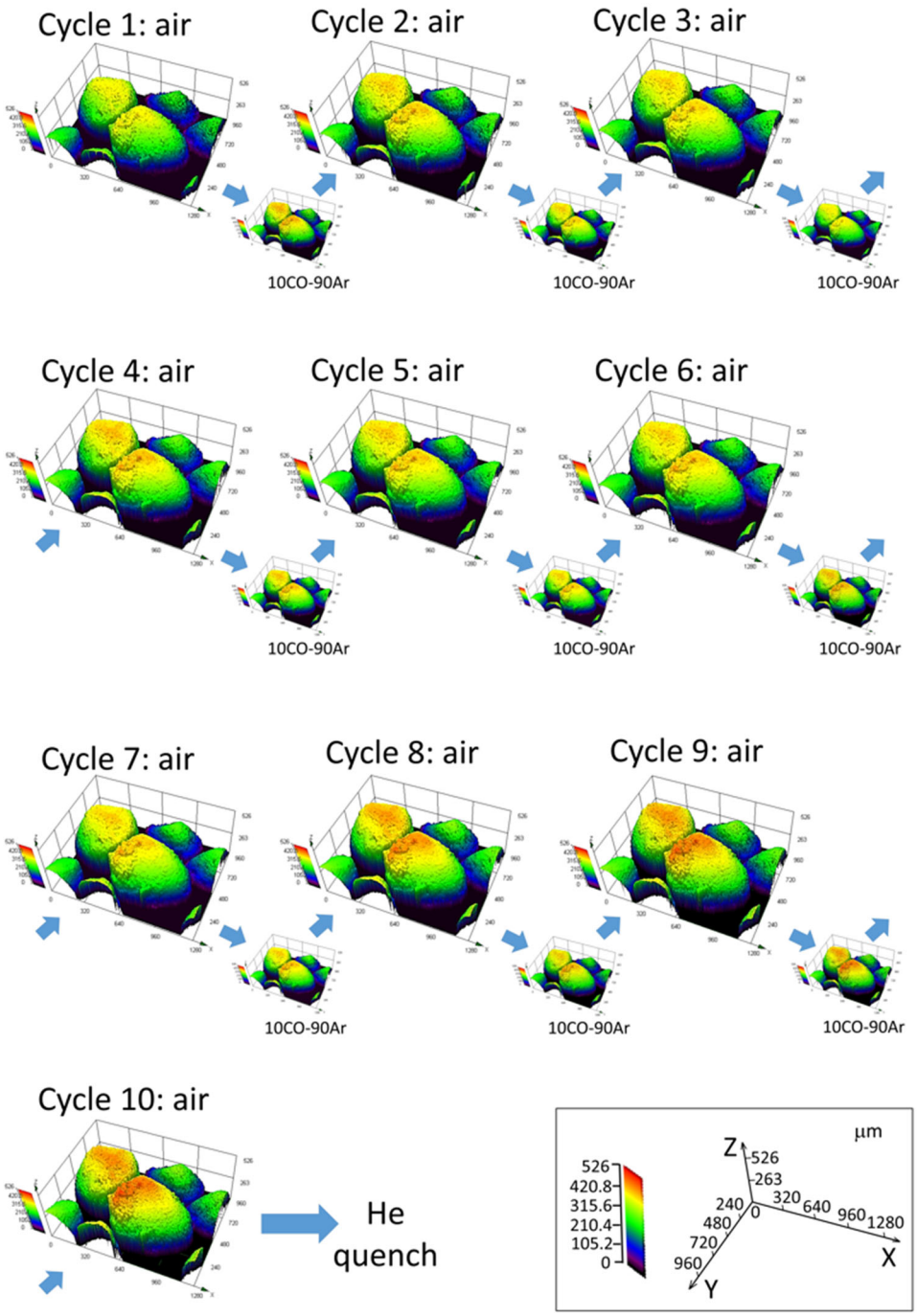

Fig. 2. Confocal laser 3D scan images of the spinel particles at 800°C at the end of each gas period (*x*, *y*, *z* scale: μm).

particle surface. The surface roughness drastically dropped during the 1st cycle and kept fluctuating between 26 μm and 35 μm. The volume change and the roughness change exhibited inverse trends. This can be attributed to particle sintering and surface morphology modification, which were occurring during redox reactions.

Electron Microscopy

The cross-sectioned particles before and after the exposures overlaid with EDX line scan data (counts for individual elements versus distance) are shown in Fig. 4. Note the inherent porosity of both samples created appreciable noise in scan results. The distributions of Al across the particle in Fig. 4 were noticeably modified after the redox exposures. In the unexposed particle, intermittent Al spikes correspond to the alumina grains supporting the spinel grains. In the exposed particle, the alumina grains became relatively smaller with less well-defined edges, following Al diffusion (likely as an ion) from the alumina grains into the spinel during the redox exposures. More frequent Al spikes for the exposed particle indicated the development of regional concentrations corresponding to Al diffusion into the Cu/Fe spinel. This will be discussed later along with Cu and Fe segregations.

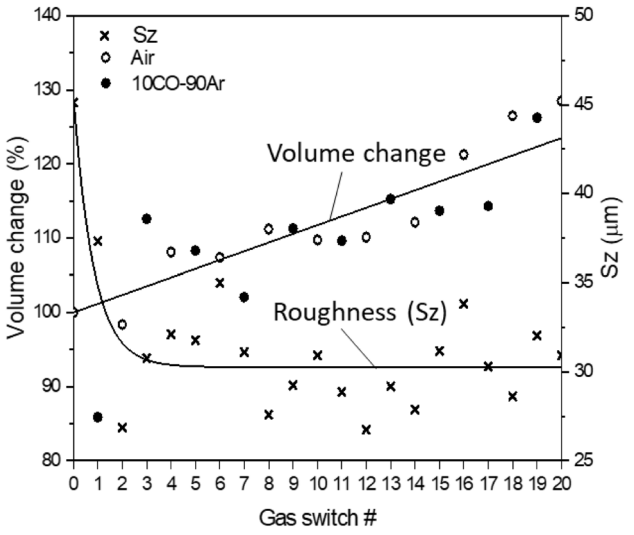

Fig. 3. Changes in volume and roughness of the spinel particles during redox cycles at 800°C. Original volume is set to be 100% at origin.

Using the image processing program, ImageJ, developed by the National Institutes of Health, the area fraction of the pores in the unexposed sample was determined to be 0.359 while the area fraction of alumina grains was 0.225, as compared to 0.182 and 0.115, respectively, for the exposed sample. The pore area fraction decreased by almost half after the redox exposures while a relative particle volume expansion of 30% was noted by the CSLM (Fig. 3). Sintering in this type of spinel may be significantly inhibited by Fe after the initial exposure to reducing conditions at high temperatures, as demonstrated by Kameoka et al.[6] The loss in alumina grain areas supports Al dissolution into the spinel at the tested temperatures.

Particle volume expansion can be explained by the formation of new phases with greater molar volumes, such as Cu metal and magnetite.[7,8] However, if the Cu/Fe spinel breaks down into $CuFeO_2$ and Cu_2O,[9] the molar volume of the product phases is less than that of the reactant phase. Another mechanism that may have driven the increase in particle volume is void formation within individual inner grains. Figure 5 shows inner grains located near the center and at the outmost edge of the spinel particle before and after the exposure. In both locations of the exposed particles, the formation of micro-voids was noted. The formation of these voids likely occurred due to diffusion of Cu and Fe from

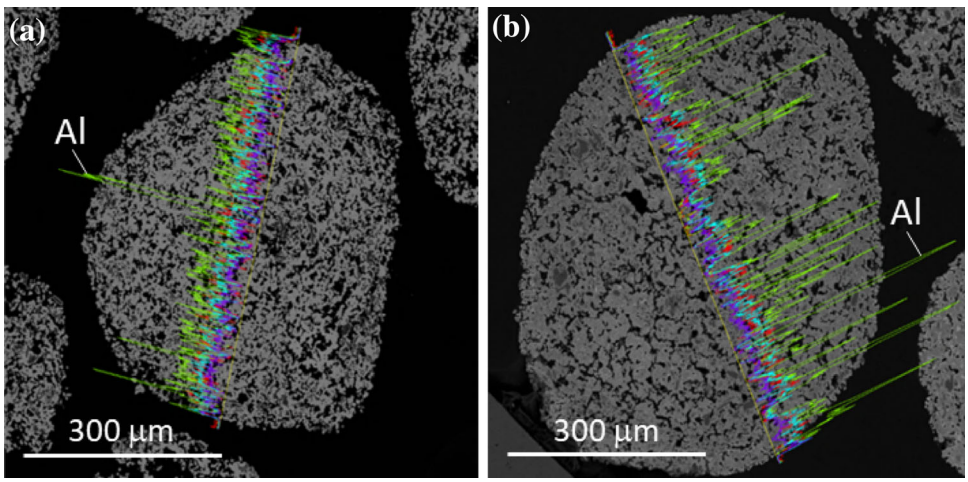

Fig. 4. SEM backscatter images of typical spinel particles overlaid with EDX line scan data (counts versus distance): (a) the unexposed sample and (b) the exposed sample.

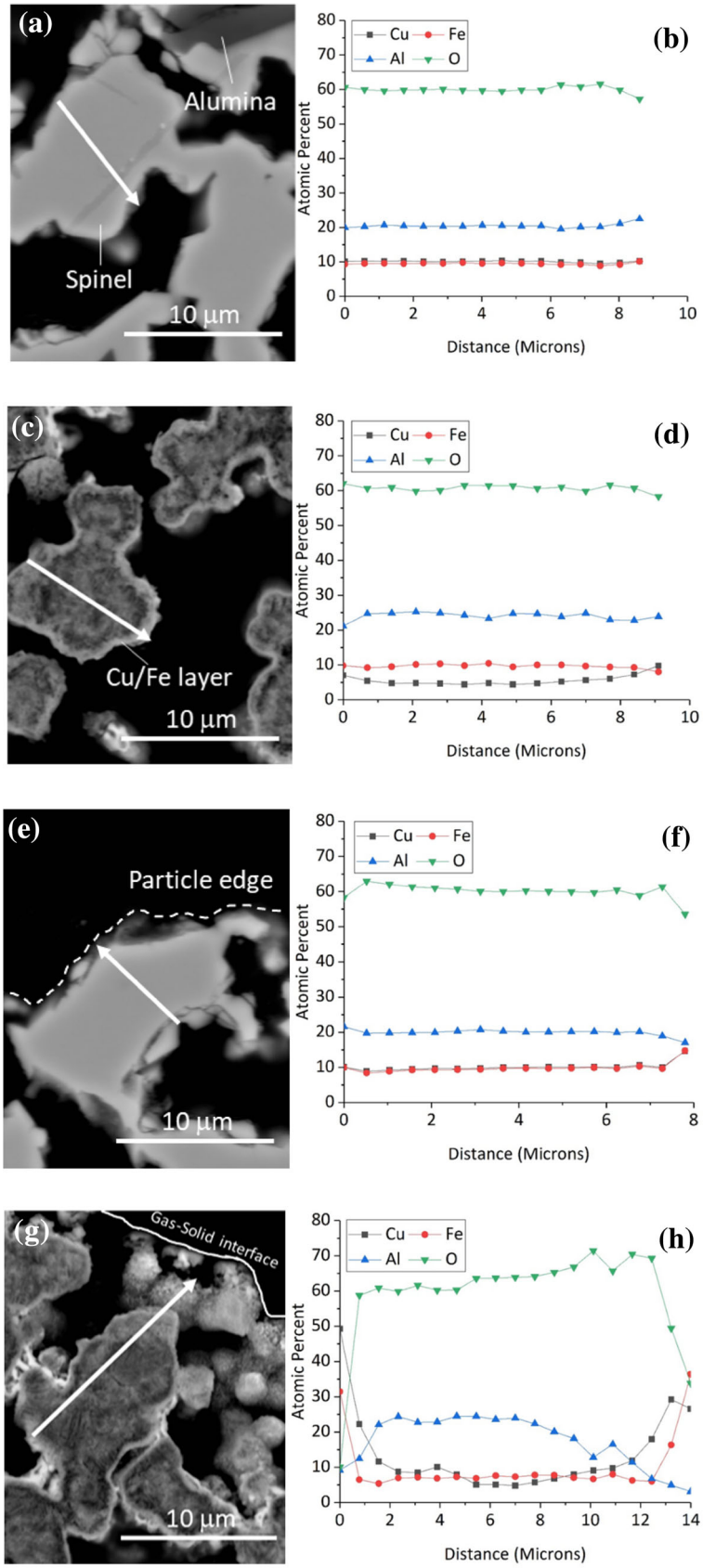

Fig. 5. SEM backscatter images and respective edge-to-edge concentration profiles across individual grains located near the center of the particle: (a, b) unexposed and (c, d) exposed; and near the edge of the particle: (e, f) unexposed and (g, h) exposed. Arrow indicates location of the line scans.

the bulk to the edges of the grains, which may have contributed to the overall particle volume expansion. A further investigation is required to understand the phenomenon. The measured area fraction of voids in the exposed sample was 0.253, compared to negligible in the unexposed sample (Fig. 5g).

Edge-to-edge concentration profiles across individual inner grains are shown in Fig. 5. A uniform element distribution can be generally noted in inner grains of the unexposed particle (Fig. 5b and f). The O concentration slightly decreases on one of the edges while those of Cu and Fe slightly increase; this was likely produced during manufacturing.

For inner grains located in the center of the exposed particle, Al dissolution from alumina to spinel can be evidenced from the abundance of Al, approximately a 5% relative increase from the unexposed grain (Fig. 5c and d). Cu migrated to the grain edges via interdiffusion, decreasing the concentration to approximately 3 at.% toward the center of the grains. Fe, in general, appeared to exhibit a similar trend to the Cu but had a slightly elevated concentration in the center. Cu and Fe segregations formed a continuous layer around the individual inner grain, which may have influenced the oxygen exchange kinetics of the particle. The segregation of Cu and Fe near the edges indicates preferential interaction with O_2 during the redox gas exposures. The differentiation was more apparent on edges adjacent to a pore (instead of another grain). The oxygen exchange at the inner grains is expected to take place by gas delivery through the pores. Overall oxygen exchange mechanisms may be different depending on grain locations within the particle, which is likely correlated to an oxygen gradient across the grain/particle, preferential redox reactions, clogging of gas passage, or a combination thereof.

The Cu and Fe segregation around the inner grains became more pronounced in the grains located closer to the outmost edge of the particle (Fig. 5g and h). Fe concentration increased from approximately 7 at.% at the middle location of the grain to approximately 32 at.% at the grain edges. A concentration gradient of Cu also increased from around 5 at.% at the middle location of the grain to as high as 50 at.% at the edge. The Al concentration, on the other hand, decreased to as low as 3 at.% at the edges.

The formation of Cu- and Fe-rich micron structures was noted on the outermost edges of the exposed particles (Fig. 5g). It was found by EDX to contain a lower level of O, indicating the potential presence of metallic species or valence change of Cu and/or Fe. Note that all the samples were exposed to air for the final 7.5 min before rapid quenching in He. A further study is underway to investigate the formation of these precipitates.

In the practice of chemical looping, oxygen carrier particles are fluidized and subjected to physical attrition. As the current particles densify over the redox cycles, the material durability is expected to improve. However, a significant increase in pore fraction in inner grains would be expected to negatively impact the mechanical properties of the material. The formation of any metallic phase around the particles would promote agglomeration during fluidizing processes at high temperature.

Individual particles can be dynamically analyzed in situ using the current real-time imaging technique, which can be applied to studies of particles with different chemistries. A combination of the environmental confocal scanning laser microscope along with SEM–EDX provides temporal and spacial insights on the qualitative and quantitative analysis of the oxygen carrier particle attrition due to chemical reactions.

The current imaging technique operates in static environments, which provides fundamental information on physical/chemical attrition. This forms a foundation for the development of oxygen carriers to be used in practical fluidized bed systems.

CONCLUSION

Structural changes of the alumina-supported Cu/Fe spinel particles in redox cycles at 800°C were studied in situ using a high-temperature confocal scanning laser microscope. Particle volume expanded with cycles while the surface roughness decreased. The volume expansion may be partly related to void formation in the inner grains caused by alumina dissolution and Cu and Fe rejection from the spinel. At the test temperature, increasing peaks in Cu concentrations at the edges of inner grains were correlated with drops in O. The measured pore area fraction of the exposed particles decreased upon the redox exposures, while that of the inner grains increased. The particle maintained its structure well during the redox cycles.

ACKNOWLEDGEMENTS

This work was performed in support of the US Department of Energy's Fossil Energy Advanced Combustion Program. The Research was executed through NETL Research and Innovation Center's Advanced Combustion effort. Research performed by AECOM Staff was conducted under the RES Contract DE-FE-0004000. Authors acknowledge Mr. M. Fortner for metallography and Mr. K. Collins for SEM.

DISCLAIMER

or process disclosed, or represents that its use would not infringe privately owned rights. Reference herein to any specific commercial product, process, or service by trade name, trademark, manufacturer, or otherwise, does not necessarily constitute or imply its endorsement, recommendation, or favoring by the United States Government or any agency thereof. The views and opinions of authors expressed herein do not necessarily state or reflect those of the United States Government or any agency thereof.

REFERENCES

1. G. Voitic and V. Hacker, *RSC Adv.* 6, 98267 (2016).
2. W. Hu, F. Donat, S.A. Scott, and J.S. Dennis, *RSC Adv.* 6, 113016 (2016).
3. W. Liu, M. Ismail, M.T. Dunstan, W. Hu, Z. Zhang, P.S. Fennell, S.A. Scott, and J.S. Dennis, *RSC Adv.* 5, 1759 (2015).
4. S. Bayham, D. Straub, and J. Weber, Operation of the NETL chemical looping reactor with natural gas and a novel copper-iron material, NETL-PUB-20912; NETL technical report series; U.S. Department of Energy, National Energy Technology Laboratory: Morgantown, WV (2017).
5. R. Siriwardane, J. Riley, S. Bayham, D. Straua, H. Tian, J. Weber, and G. Richards, *Appl. Energy* 213, 92–99 (2018).
6. S. Kameoka, T. Tanabe, and A.P. Tsai, *Catal. Lett.* 100, 89 (2005).
7. B. Wang, R. Yan, H. Zhao, Y. Zheng, Z. Liu, and C. Zheng, *Energy Fuels* 25, 3344 (2011).
8. M. Estrella, L. Barrio, G. Zhou, X. Wang, Q. Wang, W. Wen, J.C. Hanson, A.I. Frenkel, and J.A. Rodriguez, *J. Phys. Chem. C* 113, 14411 (2009).
9. K. Eguchi, N. Shimoda, K. Faungnawakij, T. Matsui, R. Kikuchi, and S. Kawashima, *Appl. Catal. B* 80, 156 (2008).